The Influence of Residence Time Distribution on Continuous-Flow Polymerization

Marcus H. Reis, Travis P. Varner, Frank A. Leibfarth*

Department of Chemistry, The University of North Carolina at Chapel Hill, Chapel Hill, NC 27599, USA

Correspondence to Frank A. Leibfarth: FrankL@email.unc.edu

ABSTRACT

Continuous-flow chemistry is emerging as an enabling technology for the synthesis of precise polymers. Despite recent advances in this rapidly growing field, there remains a need for a fundamental understanding of how fluid dynamics in tubular reactors influence polymerizations. Herein, we report a comprehensive study of how laminar flow influences polymer structure and composition. Tracer experiments coupled with in-line UV-vis spectroscopy demonstrate how viscosity, tubing diameter, and reaction time affect the residence time distribution (RTD) of fluid in reactor geometries relevant for continuous-flow polymerizations. We found that the breadth of the RTD has strong, statistical correlations with reaction conversion, polymer molar mass, and dispersity for polymerizations conducted in continuous flow. These correlations were demonstrated to be general to a variety of different reaction conditions, monomers, and polymerization mechanisms. Additionally, these findings inspired the design of a droplet flow reactor that minimizes the RTD in continuous-flow polymerizations and enables the continuous production of well-defined polymer at a rate of 1.4 kg/day.

Introduction

Continuous-flow chemistry is emerging as a useful technology for precision in polymer synthesis.[1–4] Compared to conventional batch processes, the use of micromixers and small diameter tubing leads to rapid mixing and the large specific surface area of milli-and microflow tubular reactors affords excellent heat transfer. These attributes minimize local hot spots, offer instantaneous initiation or termination of polymerizations with fast kinetics, and ultimately provide enhanced control of polymer structure and material properties.[5,6] For photocatalyzed polymerizations, small diameter flow tubing allows more uniform irradiation, faster kinetics, and easier scale-up compared to batch.[7–11] Lastly, software control of pumps, reactors, and in-line analytical techniques enables automation of polymerization processes.[12–15]

New opportunities in polymer synthesis enabled by continuous-flow chemistry include the rapid creation of polymer libraries, the telescoping of multistep polymerizations, and the automated optimization of macromolecular synthesis.[16–20] In contrast to batch processes, continuous flow's ability to dynamically alter continuous variables within a single experiment enables the rapid synthesis and analysis of polymer samples with systematic alterations in molecular weight, composition, and reaction rate. This higher-throughput approach expedites access to libraries of polymers for reaction optimization, kinetic analysis, and structure–property studies.[21,22] Continuous-flow synthesis permits users to combine multistep chemical processes into an uninterrupted sequence, which has been exploited to efficiently produce multi-block and sequence-defined copolymers.[17,23–26] Furthermore, the automation of continuous-flow polymerizations has the potential to facilitate the reproducible synthesis and analysis of synthetic polymers by non-experts, analogous to peptide synthesizers, thus removing a significant barrier to material discovery efforts.

The precise reaction conditions offered by continuous flow are especially relevant in controlled polymerizations where regulation of polymer microstructure, molecular weight, and dispersity ($Đ$) is desired. Ideally, the synergistic combination of controlled polymerizations and the well-defined reaction conditions in continuous flow would lead to polymers with predictable molar mass and low $Đ$. Studies by Yoshida, Sawamoto, and coworkers demonstrated the advantages of continuous flow for rapid and highly exothermic cationic polymerizations, where the enhanced mixing and improved heat transfer in continuous flow dramatically improved polymerization control, resulting in materials with much lower $Đ$ than analogous reactions run in batch.[27,28]

For polymerizations that exhibit slower kinetics, translation of batch reactions to continuous-flow polymerization often demonstrates poor control. In seminal work conducting reversible addition fragmentation chain-transfer (RAFT) polymerization in continuous flow, Thang *et al.* consistently observed lower monomer conversion and higher $Đ$ compared to the analogous batch reactions for a wide variety of monomers.[29] These results have been subsequently validated by a number of other independent studies and have been ascribed to fluid dynamic phenomena inherent to tubular reactors.[30–34] Fully exploiting the benefits of continuous-flow polymer synthesis will first require a fundamental understanding of how fluid dynamics in tubular reactors influence polymer structure and composition.
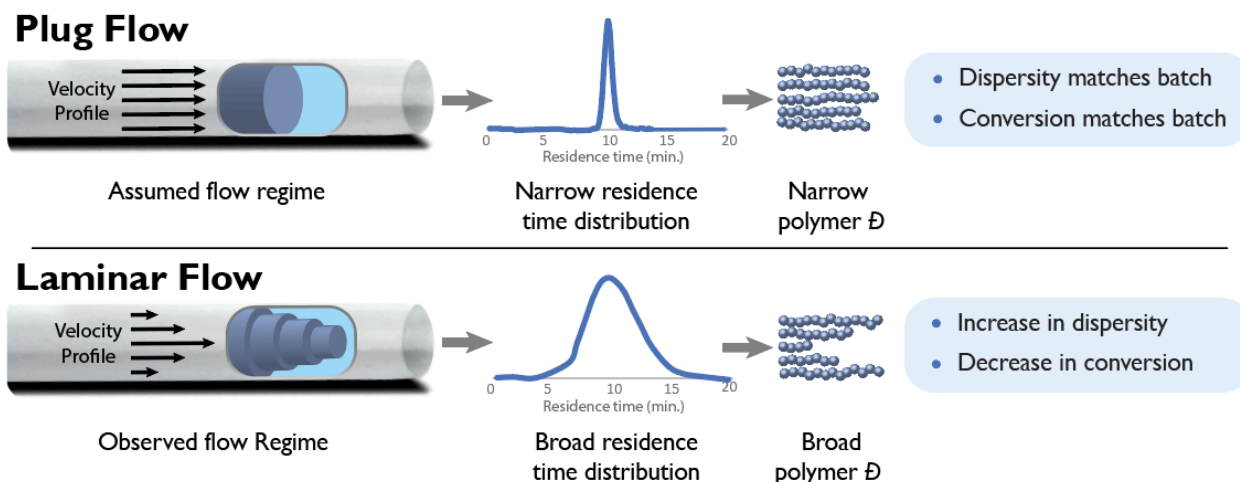
Figure 1. Comparison of different flow regimes used to describe small-diameter continuous-flow tubular reactors.

Modern polymerizations run in continuous-flow tubular reactors are predominately conducted in the laminar flow regime, which is defined as fluid moving through a closed channel with a Reynolds number less than 2000.[35] Laminar flow is characterized by ordered, parallel layers of liquid sliding past each other at different velocities with radial mixing being limited to molecular diffusion. Due to friction at the tubing-liquid interface, a parabolic velocity profile is observed with layers at the edge moving slower than layers toward the center (Figure 1). These velocity differences are maintained over long length spans due to the lack of turbulence or recirculation eddies, causing liquid to reside in the flow reactor for different amounts of time.[36–39]

The resulting residence time distribution (RTD) caused by laminar flow is defined as the distribution of time it takes simultaneously injected fluid to fully traverse and exit a flow reactor. For chemical reactions, the RTD results in a distribution in reaction time and a corresponding effect on reaction conversion and product formation.[36] For polymerizations, the RTD is directly

correlated to polymer $Đ$. Despite the emerging utility of continuous-flow polymerizations, there remains no quantitative study on how RTD influences polymer structure.

Herein, we report a comprehensive study of how laminar flow in small diameter tubular reactors influences polymer structure. Using in-line UV-vis spectroscopy, we demonstrate how tubing diameter, solution viscosity, and mean residence time influence RTD under conditions relevant for continuous-flow polymerization. We subsequently conduct polymerizations under various conditions and reactor geometries to understand how RTD influences reaction conversion, polymer molar mass (M_n), and $Đ$. The breadth of the RTD in laminar flow is found to have strong, statistical correlations with polymerization control. These correlations are demonstrated to be general to a variety of different reaction conditions, monomers, and polymerization mechanisms. Additionally, our comprehensive studies have enabled the rational design of a reactor to minimize RTD, enabling the continuous production of well-defined polymer at a rate of 1.4 kg/day.

Results and Discussion

The effect of reactor geometry on experimentally measured RTD. Reports of polymerizations conducted in continuous flow have typically assumed plug flow as a simplified model of solution moving through a reactor. In plug flow, fluid velocity is assumed to be constant across any cross-section of the tubular reactor and no boundary layer is considered at the fluid–wall interface.[35] The RTD of plug flow is assumed to be negligible (Figure 1). In reality, continuous-flow polymerizations are conducted in tubular reactors at low to moderate flow rates under laminar flow conditions, where solution in the middle of the tube exits the reactor faster than the mean residence time and solution near the walls resides in the reactor much longer.
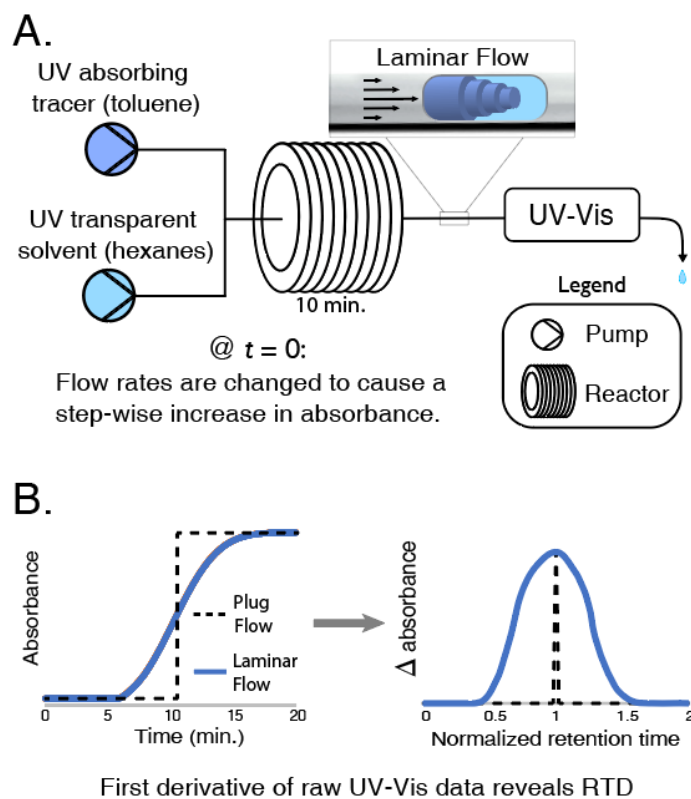
Figure 2. A. Continuous-flow setup used to measure residence time distribution (RTD); **B**. Analysis of UV-Vis response allows experimental determination of RTD.

To experimentally measure the RTD of common flow geometries, in-line UV-vis spectroscopy was used to track the dispersion of an injected tracer. A flow system was first brought to steady state operation before a UV-absorbing small molecule tracer was introduced into the system (Figure 2A). The RTD was extracted from absorbance measurements in the time between when the tracer first begins exiting the reactor and the absorbance reaches a new steady state (Figure 2B). In a typical experiment, the observed RTD was calculated for a specific tubing diameter or flow rate, with hexanes as the mobile phase and toluene as the UV-absorbing small molecule tracer. To probe the effect of viscosity on RTD, the identity of the mobile phase was changed from hexanes (0.3 mPa*s) to either a 90% acetonitrile-water solution (0.5 mPa*s), water

(1 mPa*s), a 9% polyethylene glycol-water solution (9.1 mPa*s), or a 23% polyethylene glycol-water solution (85 mPa*s). For aqueous solutions the absorbing tracer was changed from toluene to phenol. These experiments enabled visualization of the influence of tubing diameter, residence time, and molecular diffusion on the RTD under conditions commonly used for continuous-flow polymerizations (Figure 3). In agreement with previous studies, increasing tubing size, decreasing retention time, and increasing viscosity all resulted in a broadening of RTD.[36]
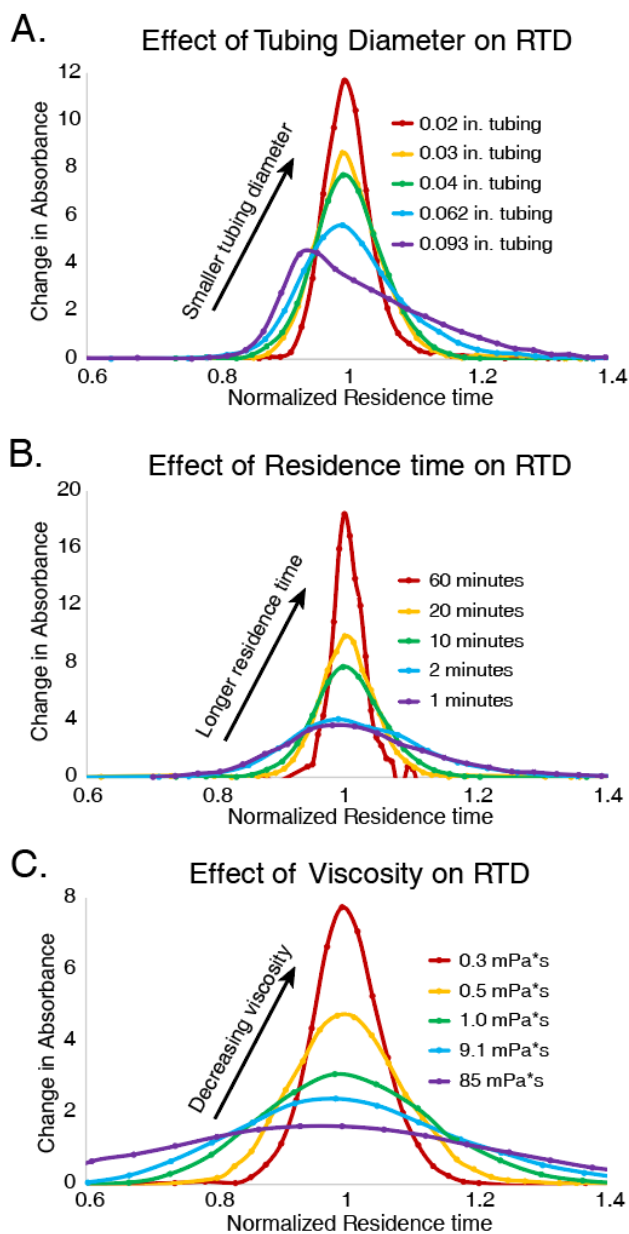
Figure 3. Experimental RTD of common continuous-flow conditions using small molecule tracers. The area under the curve has been normalized to one. **A**. Effect of tubing diameter on RTD with constant retention time and viscosity (10 min. and 0.3 mPa*s, respectively). **B**. Effect of retention time on RTD with constant tubing diameter and viscosity (0.04 in. and 0.3 mPa*s, respectively). **C**. Effect of viscosity on RTD with constant tubing diameter and retention time (0.04 in. and 10 min., respectively). Flow rates for each condition is detailed in the Supporting Information.

We hypothesized that the RTD of a growing polymer would deviate from that of small molecule tracers. To test this hypothesis on a model system, we chose to explore the ring-opening transesterification polymerization (ROTP) of γ-valerolactone (γ-VL) catalyzed by 1,5,7-triazabicyclo[4.4.0]dec-5-ene (TBD). The polymerization in flow was first brought to steady state operation using hexanol as an initiator. Subsequent replacement of hexanol with pyrenebutanol by a step change in flow rate of two pumps provided a polymer-bound UV–Vis tracer while keeping the total concentration of alcohol constant. The resulting RTD observed for an active polymerization (Figure 4) is much broader than analogous experiments conducted with small molecule tracers under otherwise identical conditions. While the small molecule experiments in Figure 3 demonstrated a symmetric RTD that is predicted by the dispersion model of fluid transport in a tubular reactor, a convective model of fluid transport more accurately describes the asymmetric RTD seen in polymerizations.[37] This convective model is typically observed in flow geometries with minimal radial diffusive mixing or large tubing diameters (Figure 3A). We predict that the slower molecular diffusion of polymer chains as well as the inherent viscosity of polymer solutions leads to convective fluid transport even in small diameter tubing, resulting in a broader RTD than previously studied small molecule systems.
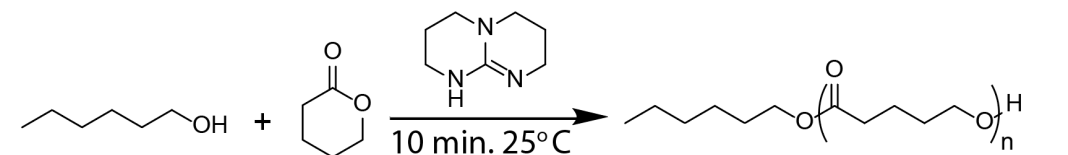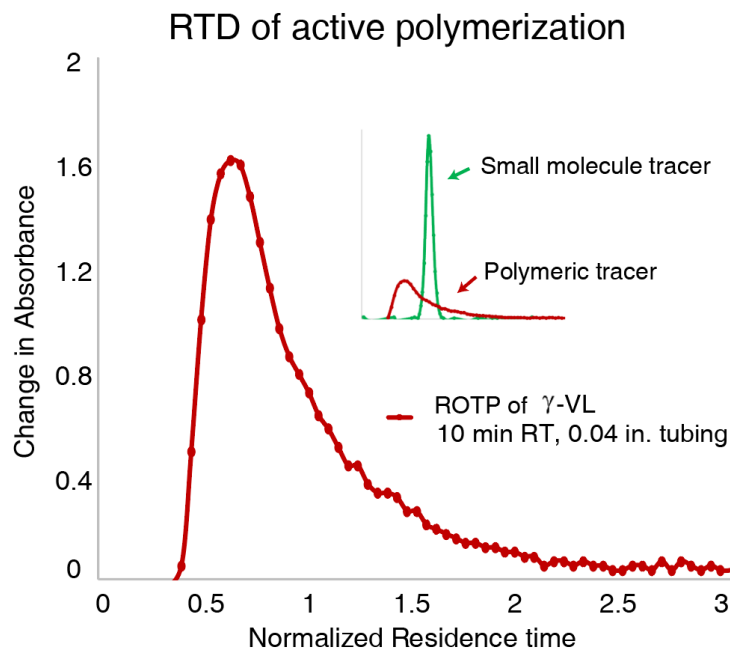
8

Figure 4. Comparison between the observed RTD of a polymerization and a small molecule model experiment under the same reaction geometry (10 min. residence time and 0.04 in. tubing).

The influence of RTD on polymerization performance. Quantifying the influence of RTD on monomer conversion, M_n, and $Đ$ for continuous-flow polymerization is non-trivial. Viscosity constantly evolves as a polymerization progresses and different retention times have a non-linear effect on reaction conversion. Therefore, the modification of tubing diameter was chosen as a user-defined variable to enable the systematic study of RTD's effect on polymer structure. Model studies with small molecule tracers (Figure 3A) demonstrated that increasing tubing diameter increases the RTD; thus, we hypothesized that an increase in tubing diameter in a continuous-flow polymerization would result in a decrease in conversion, decrease in M_n, and increase in $Đ$. The controlled ROTP of γ-VL was carried out in reactors with tubing inner-diameters of 0.02 in., 0.03 in., 0.04 in., 0.063 in., and 0.093 in. As a control, these results were

9

compared to a polymerization run in a small scale (2 mL) batch reactor, which had sufficiently fast

mixing and heat transfer to approximate an experiment with no RTD.

Reactor geometry[b]	M_n (g/mol)[c]	Đ[c]	Conversion (%)[d]
Batch (2 mL scale)	11,200 ± 200	1.05 ± 0.01	69 ± 9
Flow (0.02 in. tubing)	11,300 ± 900	1.12 ± 0.01	69 ± 2
Flow (0.03 in. tubing)	11,000 ± 400	1.14 ± 0.04	63 ± 3
Flow (0.04 in. tubing)	10,800 ± 500	1.15 ± 0.01	62 ± 2
Flow (0.063 in. tubing)	9,000 ± 300	1.27 ± 0.07	50 ± 5
Flow (0.093 in. tubing)	9,000 ± 1,000	1.33 ± 0.06	49 ± 8

Table 1. Continuous-flow polymerization of γ-VL with varied tubing diameters. Reactions were

conducted in triplicate and the standard deviations are reported. [a]Conditions: [γ-VL] = 5M; [γ-

VL]:[initiator]:[TBD] = [125]:[1]:[0.4]; Theoretical M_n at 100% conversion = 25,600 g/mol.

[b]Tubing lengths and flow rates found in SI. [c]Measured by GPC using polystyrene standards.

[d]Determined by ^{1}H NMR.

    As shown in Table 1, the RTD in laminar flow led to decreased control compared to an

analogous small-scale batch reaction, with clear correlations observed between tubing diameter,

conversion, M_n, and Đ. Each experiment was conducted three times and standard deviations are

reported in Table 1. Even in the smallest inner-diameter tubing tested, Đ increased from 1.05 in

batch to 1.12 in flow, and increases in tubing inner-diameter led to further increases in Đ. In the

largest diameter tubing (0.093 in.), both conversion and M_n decreased 20% compared to batch and

Đ increased from 1.05 to 1.33. These results represent a significant limitation for the scale-up of

continuous-flow polymerizations, since large tubing inner-diameters enable higher continuous

throughput for a given reaction. We note that large scale polymerizations in batch also deviate from ideal behavior due to poor mass and heat transfer in larger volume batch reactors.

Overcoming RTD with droplet flow. The combined UV-Vis and polymerization data suggest that decreasing tubing diameter, increasing retention time, and decreasing viscosity result in better control. For polymerizations run in continuous flow, however, the pressure drop along a given length of tubing must be considered concomitantly with changes to the reactor geometry. Pressure drop (ΔP) is the result of frictional forces between the stationary tubing and the moving liquid and can be quantified by the Hagen-Poiseuille equation[35]:

$$\Delta P = \frac{128\mu L Q}{\pi d_t^4}$$

Where, μ is the dynamic viscosity, L the tubing length, Q the volumetric flow rate, and d_t the tubing diameter. For polymerizations conducted in continuous flow, pressure drop commonly becomes high enough to stall pumps or burst tubing due the increasing viscosity of the polymerizing mobile phase. Strategies to mitigate the negative impacts of laminar flow on polymer structure and Đ also exaggerate pressure drop within the flowing system. For example, diluting the reaction will lower the pressure drop, but requires a faster flow rate (Q) and longer lengths of tubing (L) to maintain an equal throughput. Similarly, decreasing tubing inner-diameter (d_t) exponentially increases pressure drop and increases the difficulty of producing samples in a meaningful quantity. For these reasons, we found it challenging to use the aforementioned techniques to minimize RTD and replicate the control observed in small-scale batch polymerizations.

Two alternative techniques to minimize the RTD in tubular microreactors include the creation of Dean vortices or the use of in-line static mixers.[40,41] Dean vortices represent secondary

fluid motion in laminar flow resulting from centripetal forces of fluid flowing in tubes arranged with tight curvature. Tracer experiments on both tightly and loosely coiled reactors showed no difference in RTD, suggesting that Dean vortices did not occur in the geometries and reaction conditions explored herein. The use of static mixers is a potential solution, but they exaggerate ΔP, are prone to clog with viscous solutions, and require optimization for each system.

Gas–liquid segmented flow, also referred to as Taylor flow or droplet flow,[42] is an alternative and attractive approach to decrease the RTD in continuous-flow reactors. The droplet flow approach compartmentalizes slugs of liquid in an immiscible mobile phase (Figure 5). Within each slug, recirculation motions enhance mixing and the lack of slug coalescence ensures a narrow RTD. This approach has been shown to narrow the RTD of both small molecule reactions and nanoparticle synthesis, for the latter decreasing the size dispersity of nanoparticles formed in droplet flow compared to continuous flow.[43–45]

Using a metering valve and an inert gas, we evaluated the influence of droplet flow on the RTD of continuous-flow polymerizations. Tracer experiments analyzed by in-line UV-vis spectroscopy were used quantify the RTD of viscous fluids in droplet flow. For the most viscous sample analyzed in Figure 3C (85 mPa•s), droplet flow resulted in a narrower RTD than even the analogous non-viscous sample (0.3 mPa*s) run in traditional continuous flow.
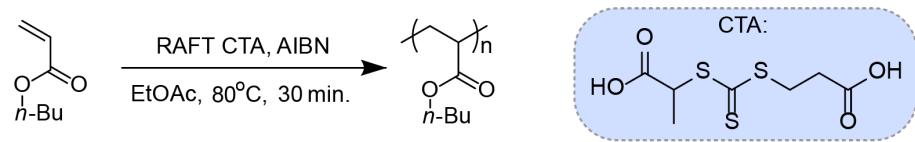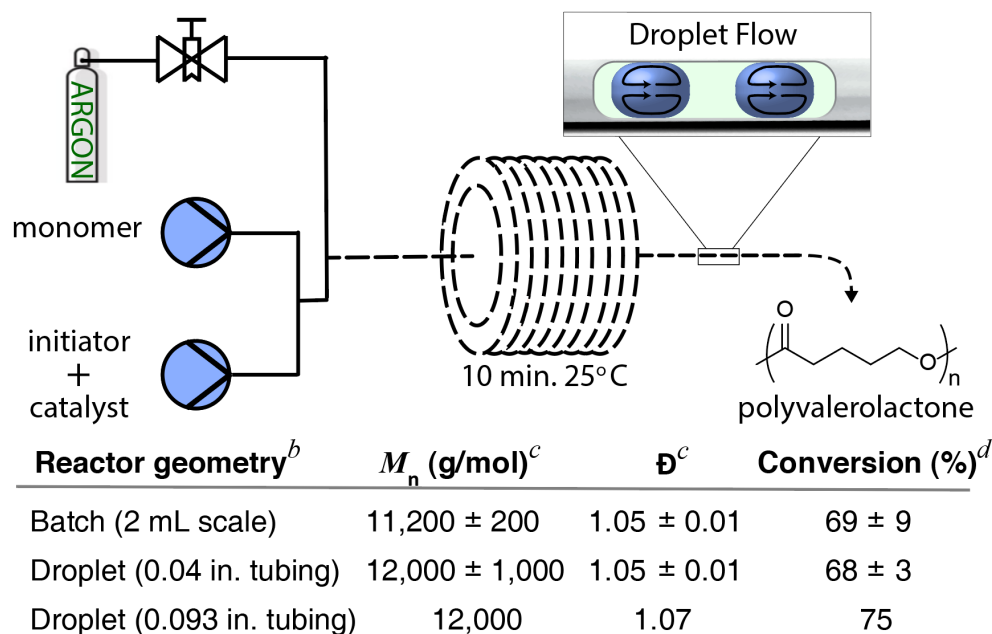
Reactor geometry[b]	M_n (g/mol)[c]	$Đ$[c]	Conversion (%)[d]
Batch (2 mL scale)	11,200 ± 200	1.05 ± 0.01	69 ± 9
Droplet (0.04 in. tubing)	12,000 ± 1,000	1.05 ± 0.01	68 ± 3
Droplet (0.093 in. tubing)	12,000	1.07	75

Figure 5. Polymerization of γ-VL using droplet flow. The reaction run in 0.093 in. inner diameter tubing produced poly(γ-VL) at a rate of 1.4 kg/day. [a]Conditions: [γ-VL] = 5M; [γ-VL]:[initiator]:[TBD] = [125]:[1]:[0.4]; Theoretical M_n at 100% conversion = 25,600 g/mol. [b]Tubing lengths and flow rates found in SI. [c]Measured by GPC using polystyrene standards. [d]Determined by ^{1}H NMR.

The polymerization of γ-VL was used to probe the influence of droplet flow on polymerization (Figure 5). Droplet flow demonstrated a dramatic improvement compared to analogous continuous-flow polymerizations. Even in the largest diameter tubing, the conversion, M_n, and $Đ$ all effectively matched that of a small-scale batch reaction. The improvement in RTD was found to be decoupled from retention time, viscosity, and tubing diameter, thus overcoming a crucial hurdle for continuous-flow polymerizations. Using two peristaltic pumps at a total flow rate of 3.6 mL/s and 0.093 in. inner-diameter tubing, the polymerization of γ-VL was scaled up to collect poly(γ-VL) continuously at a rate that would equate to 1.4 kg/day under continuous operation. Importantly, both the M_n (12.0 kg/mol) and $Đ$ (1.07) of the polymer was analogous to a

small-scale batch polymerization. A built-in pressure monitoring system demonstrated that total system pressure never exceeded 5 pounds-per-square-inch, indicating that further scale-up is possible.

In order to probe the generality of RTD's effects, we studied the RAFT polymerization of *n*-butyl acrylate (*n*BuA), *N*-isopropylacrylamide (NIPAM) and *N,N*-dimethylacrylamide (DMA). These studies expanded the data set from ROTP to controlled radical polymerization while simultaneously investigating polymerizations with both slower (*n*BuA) and faster (NIPAM and DMA) reaction kinetics. The RAFT polymerization of *n*BuA was studied at a retention time of 30 minutes (Figure 6). The polymerization run in batch resulted in poly(*n*BuA) with a M_n of 13.0 kg/mol and a *Đ* of 1.14. Polymerizations run in continuous flow demonstrated a correlation between increasing tubing diameter and increasing *Đ*. This loss of polymerization control is consistent with the results observed with poly(γ-VL) (Table 1). We hypothesize that the magnitude of *Đ* change is less for the slower polymerization of *n*BuA due to the narrower RTD observed for reactions with longer residence times (Figure 3B). The polymerization of *n*BuA, however, did not demonstrate a reduction in monomer conversion with increasing tubing diameter. While we have limited experimental evidence at the current time, we hypothesize that the broadening of *Đ* without the associated decrease in monomer conversion is due to the differences in the RTD of the monomers and growing polymer chains in solution. Due to differences in molecular diffusion, a narrower RTD is expected for unreacted monomers as compared to the growing polymer chains, especially at longer residence times (Figure. 4). This would lead to the RTD in this system having a smaller impact on monomer conversion as compared to polymer *Đ*.

Reactor geometry[b]	M_n (g/mol)[c]	$Đ$[c]	Conversion (%)[d]
Batch (2 mL scale)	13,400	1.14	62
Flow (0.04 in. tubing)	13,100	1.17	64
Flow (0.093 in. tubing)	13,100	1.26	65
Droplet (0.093 in. tubing)	13,600	1.15	60

Table 2. Continuous-flow polymerization of nBuA with varied tubing diameters. [a]Conditions: [nBuA] = 2M; [nBuA]:[CTA]:[AIBN] = [200]:[1]:[0.3]; Theoretical M_n at 100% conversion = 25,600 g/mol. [b]Tubing lengths and flow rates found in SI. [c]Measured by GPC using polystyrene standards. [d]Determined by ^{1}H NMR.

Expected trends were observed for the polymerization of NIPAM at a five-minute retention time, with droplet flow leading to an even lower $Đ$ than that observed in an analogous batch experiment (additional polymerization data can be found in the SI). The polymerization of DMA, however, demonstrated additional complexities of running polymerizations in continuous flow beyond RTD. For this polymerization exhibiting rapid kinetics, heat transfer and mixing were found to have significantly larger effects on conversion and $Đ$ than RTD. For example, in two otherwise identical reactions, conversion in a 2 mL batch reactor was increased from 6% to 87% upon preheating the monomer solution prior to adding the thermal initiator, highlighting the slow heat transfer in batch. The analogous flow reaction achieved a moderate conversion of 64% without any preheating. Surprisingly, attempts to preheat the flow reaction by separating the monomer and initiator solutions into two syringes and recombining them using a T-mixer led to a decrease in conversion and an increase in $Đ$. The collection of these experimental observations suggests that mixing, not reactor geometry, is the primary determinant to achieve controlled

polymerizations in flow with monomers that exhibit rapid kinetics. For fast reactions in flow, improving mixing efficiency through the use of more advanced micromixers is suggested, and a number of quality discussions on the topic can be found elsewhere.[36,37]

Conclusion

We have provided experimental evidence that the RTD associated with laminar flow in tubular microreactors has strong, statistical correlations with reaction conversion, M_n, and $Đ$ in continuous-flow polymerizations. Tracer experiments coupled with in-line UV-vis spectroscopy demonstrated that decreasing retention time, increasing viscosity, and increasing tubing diameter resulted in broadening of the RTD. For the ROTP of γ-VL, we found that the broadening of the RTD directly correlated to an increase in $Đ$ and a decrease in both M_n and conversion. Droplet flow was discovered as a solution to mitigate the negative effects of RTD for the continuous-flow polymerization of γ-VL, resulting in a method that matched the results of a small-scale batch reaction while producing narrowly disperse polymer ($Đ$ = 1.07) at a rate of 1.4 kg/day. Furthermore, these observations were generalized to polymerizations with different mechanisms and different reaction rates. The fundamental understanding of laminar flow's influence on polymerization detailed herein will facilitate the broader adoption of continuous-flow synthesis in polymer science.

ASSOCIATED CONTENT

Detailed information on reagents, analytic instrumentation, specific reactor tubing specifications, flow rates, list of commercially available flow equipment, specific procedures for the polymerizations of δ-valerolactone, *n*-butyl acrylate, *N*-isopropylacrylamide, and *N,N*-dimethylacrylamide, extended polymerization data of poly(*n*-butyl acrylate), poly(N-

isopropylacrylamide), poly(*N*,*N*-dimethylacrylamide) and explanation of data workup for residence time distribution visualizations can be found in the Supporting Information.

AUTHOR INFORMATION

Corresponding Authors

*E-mail: FrankL@email.unc.edu

Notes: The authors declare no competing financial interest.

References:

(1) Tonhauser, C.; Natalello, A.; Lo, H.; Frey, H. Micro Flow Technology in Polymer Synthesis. *Macromolecules* **2012**, *45*, 9551–9570.

(2) Myers, R. M.; Fitzpatrick, D. E.; Turner, R. M.; Ley, S. V. Flow Chemistry Meets Advanced Functional Materials. *Chem. - A Eur. J.* **2014**, 12348–12366.

(3) Plutschack, M. B.; Pieber, B.; Gilmore, K.; Seeberger, P. H. The Hitchhiker's Guide to Flow Chemistry. *Chem. Rev.* **2017**, *117* (18), 11796–11893.

(4) Junkers, T. Precise Macromolecular Engineering via Continuous-Flow Synthesis Techniques. *J. Flow Chem.* **2017**, *7*, 106–110.

(5) Junkers, T. Precision Polymer Design in Microstructured Flow Reactors: Improved Control and First Upscale at Once. *Macromol. Chem. Phys.* **2017**, *218* (2), 1–9.

(6) Iwasaki, T.; Yoshida, J.-I. Free Radical Polymerization in Microreactors. Significant Improvement in Molecular Weight Distribution Control. *Macromolecules* **2005**, *38*, 1159–

1163.

(7)   Chen, M.; Zhong, M.; Johnson, J. A. Light-Controlled Radical Polymerization: Mechanisms, Methods, and Applications. *Chem. Rev.* **2016**, *116*, 10167–10211.

(8)   Melker, A.; Fors, B. P.; Hawker, C. J.; Poelma, J. E. Continuous Flow Synthesis of Poly(Methyl Methacrylate) via a Light-Mediated Controlled Radical Polymerization. *J. Polym. Sci. Part A Polym. Chem.* **2015**, *53*, 2693–2698.

(9)   Wenn, B.; Conradi, M.; Carreiras, A. D.; Haddleton, D. M.; Junkers, T. Photo-Induced Copper-Mediated Polymerization of Methyl Acrylate in Continuous Flow Reactors. *Polym. Chem.* **2014**, *5*, 3053–3060.

(10)   Corrigan, N.; Rosli, D.; Jones, J. W. J.; Xu, J.; Boyer, C. Oxygen Tolerance in Living Radical Polymerization: Investigation of Mechanism and Implementation in Continuous Flow Polymerization. *Macromolecules* **2016**, *49*, 6779–6789.

(11)   Ramsey, B. L.; Pearson, R. M.; Beck, L. R.; Miyake, G. M. Photoinduced Organocatalyzed Atom Transfer Radical Polymerization Using Continuous Flow. *Macromolecules* **2017**, *50*, 2668–2674.

(12)   Rubens, M.; Vrijsen, J. H.; Laun, J.; Junkers, T. Precise Polymer Synthesis by Autonomous Self-Optimizing Flow Reactors. *Angew. Chemie Int. Ed.* **2018**, *57*, 1–6.

(13)   Bally, F.; Serra, C. A.; Brochon, C.; Anton, N.; Vandamme, T.; Hadziioannou, G. A Continuous-Flow Polymerization Microprocess with Online GPC and Inline Polymer Recovery by Micromixer-Assisted Nanoprecipitation. *Macromol. React. Eng.* **2011**, *5* (11–12), 542–547.

(14)   Bédard, A.-C.; Adamo, A.; Aroh, K. C.; Grace Russell, M.; Bedermann, A. A.; Torosian, J.; Yue, B.; Jensen, K. F.; Jamison, T. F. Reconfigurable System for Automated

Optimization of Diverse Chemical Reactions. *Science* . **2018**, *361*, 1220–1225.

(15)   Haven, J. J.; Junkers, T. Online Monitoring of Polymerizations: Current Status. *European J. Org. Chem.* **2017**, 6474–6482.

(16)   Hornung, C. H.; von Känel, K.; Martinez-Botella, I.; Espiritu, M.; Nguyen, X.; Postma, A.; Saubern, S.; Chiefari, J.; Thang, S. H. Continuous Flow Aminolysis of RAFT Polymers Using Multistep Processing and Inline Analysis. *Macromolecules* **2014**, *47* (23), 8203–8213.

(17)   Corrigan, N.; Manahan, R.; Lew, Z. T.; Yeow, J.; Xu, J.; Boyer, C. Copolymers with Controlled Molecular Weight Distributions and Compositional Gradients through Flow Polymerization. *Macromolecules* **2018**, *51*, 4553–4563.

(18)   Rosenfeld, C.; Serra, C.; O'Donohue, S.; Hadziioannou, G. Continuous Online Rapid Size Exclusion Chromatography Monitoring of Polymerizations - CORSEMP. *Macromol. React. Eng.* **2007**, *1*, 547–552.

(19)   Reis, M. H.; Davidson, C. L. G.; Leibfarth, F. A. Continuous-Flow Chemistry for the Determination of Comonomer Reactivity Ratios. *Polym. Chem.* **2018**, *9*, 1728–1734.

(20)   Corrigan, N.; Almasri, A.; Taillades, W.; Xu, J.; Boyer, C. Controlling Molecular Weight Distributions through Photoinduced Flow Polymerization. *Macromolecules* **2017**, *50* (21), 8438–8448.

(21)   Brocken, L.; Price, P. D.; Whittaker, J.; Baxendale, I. R. Continuous Flow Synthesis of Poly(Acrylic Acid) via Free Radical Polymerisation. *React. Chem. Eng* **2017**, *2*, 662–668.

(22)   Krishnadasan, S.; Brown, R. J. C.; Demello, A. J.; Demello, J. C. Intelligent Routes to the Controlled Synthesis of Nanoparticles. *Lab Chip* **2007**, *7*, 1434–1441.

(23)   Kuroki, A.; Martinez-Botella, I.; Hornung, C. H.; Martin, L.; Williams, E. G. L.; Locock,

K. E. S.; Hartlieb, M.; Perrier, S. Looped Flow RAFT Polymerization for Multiblock Copolymer Synthesis. *Polym. Chem.* **2017**, *8*, 3249–3254.

(24) Zhu, N.; Feng, W.; Hu, X.; Zhang, Z.; Fang, Z.; Zhang, K.; Li, Z.; Guo, K. Organocatalyzed Continuous Flow Ring-Opening Polymerizations to Homo- and Block-Polylactones. *Polymer.* **2016**, *84*, 391–397.

(25) Wicker, A. C.; Leibfarth, F. A.; Jamison, T. F. Flow-IEG Enables Programmable Thermodynamic Properties in Sequence-Defined Unimolecular Macromolecules. *Polym. Chem.* **2017**, *8*, 5786-5794.

(26) Baeten, E.; Haven, J. J.; Junkers, T. RAFT Multiblock Reactor Telescoping: From Monomers to Tetrablock Copolymers in a Continuous Multistage Reactor Cascade. *Polym. Chem.* **2017**, *8* (25), 3815–3824.

(27) Nagaki, A.; Iwasaki, T.; Kawamura, K.; Yamada, D.; Suga, S.; Ando, T.; Sawamoto, M.; Yoshida, J. Microflow System Controlled Carbocationic Polymerization of Vinyl Ethers. *Chem. - An Asian J.* **2008**, *3*, 1558–1567.

(28) Nagaki, A.; Kawamura, K.; Suga, S.; Ando, T.; Sawamoto, M.; Yoshida, J. I. Cation Pool-Initiated Controlled/Living Polymerization Using Microsystems. *J. Am. Chem. Soc.* **2004**, *126* (45), 14702–14703.

(29) Hornung, C. H.; Guerrero-Sanchez, C.; Brasholz, M.; Saubern, S.; Chiefari, J.; Moad, G.; Rizzardo, E.; Thang, S. H. Controlled RAFT Polymerization in a Continuous Flow Microreactor. *Org. Process Res. Dev.* **2011**, *15*, 593–601.

(30) Paulus, R. M.; Erdmenger, T.; Becer, C. R.; Hoogenboom, R.; Schubert, U. S. Scale-Up of Microwave-Assisted Polymerizations in Continuous-Flow Mode: Cationic Ring-Opening Polymerization of 2-Ethyl-2-Oxazoline. *Macromol. Rapid Commun.* **2007**, *28*, 484–491.

(31)   Russum, J. P.; Jones, C. W.; Schork, F. J. Continuous Reversible Addition-Fragmentation Chain Transfer Polymerization in Miniemulsion Utilizing a Multi-Tube Reaction System. *Macromol. Rapid Commun.* **2004**, *25*, 1064–1068.

(32)   Wurm, F.; Wilms, D.; Klos, J.; Löwe, H.; Frey, H. Carbanions on Tap – Living Anionic Polymerization in a Microstructured Reactor. *Macromol. Chem. Phys.* **2008**, *209* (11), 1106–1114.

(33)   Iida, K.; Chastek, T. Q.; Beers, K. L.; Cavicchi, K. A.; Chun, J.; Fasolka, M. J. Living Anionic Polymerization Using a Microfluidic Reactor. *Lab Chip* **2009**, *9*, 339–345.

(34)   Diehl, C.; Laurino, P.; Azzouz, N.; Seeberger, P. H. Accelerated Continuous Flow RAFT Polymerization. *Macromolecules* **2010**, *43*, 10311–10314.

(35)   Spurk, J. H.; Aksel, N. *Fluid Mechanics*, Second edi.; Springer, 2008.

(36)   Nagy, K. D.; Shen, B.; Jamison, T. F.; Jensen, K. F. Mixing and Dispersion in Small-Scale Flow Systems. *Org. Process Res. Dev.* **2012**, *16*, 976–981.

(37)   Gobert, S. R. L.; Kuhn, S.; Braeken, L.; Thomassen, L. C. J. Characterization of Milli-and Microflow Reactors: Mixing Efficiency and Residence Time Distribution. *Org. Process Res. Dev.* **2017**, *21*, 531–542.

(38)   Levenspiel, O.; Smith, W. K. Notes on the Diffusion-Type Model for the Longitudinal Mixing of Fluids in Flow. *Chem. Engng Sci.* **1957**, *6*, 227–233.

(39)   Taylor, G. Dispersion of Soluble Matter in Solvent Flowing Slowly through a Tube. *Proc. R. Soc. A Math. Phys. Eng. Sci.* **1953**, *219* (1137), 186–203.

(40)   Nivedita, N.; Ligrani, P.; Papautsky, I. Dean Flow Dynamics in Low-Aspect Ratio Spiral Microchannels. *Sci. Rep.* **2017**, *7*, 1–10.

(41)   Lueth, F. G.; Pauer, W.; Moritz, H.-U. Properties of Smart-Scaled PTFE-Tubular Reactors

for Continuous Emulsion Polymerization Reactions. *Macromol. Symp.* **2013**, *333*, 69–79.

(42) Song, H.; Chen, D. L.; Ismagilov, R. F. Reactions in Droplets in Microfluidic Channels. *Angew. Chemie Int. Ed.* **2006**, *45* (44), 7336–7356.

(43) Cabeza, V. S.; Kuhn, S.; Kulkarni, A. A.; Jensen, K. F. Size-Controlled Flow Synthesis of Gold Nanoparticles Using a Segmented Flow Microfluidic Platform. *Langmuir* **2012**, *28*, 7007–7013.

(44) Yen, B. K. H.; Günther, A.; Schmidt, M. A.; Jensen, K. F.; Bawendi, M. G. A Microfabricated Gas-Liquid Segmented Flow Reactor for High-Temperature Synthesis: The Case of CdSe Quantum Dots. *Angew. Chemie Int. Ed.* **2005**, *44*, 5447–5451.

(45) Köhler, J. M.; Li, S.; Knauer, A. Why Is Micro Segmented Flow Particularly Promising for the Synthesis of Nanomaterials? *Chem. Eng. Technol.* **2013**, *36*, 887–899.

Supporting Information

The Influence of Residence Time Distribution on Continuous-Flow Polymerization

Marcus H. Reis, Travis P. Varner, and Frank A. Leibfarth*

Department of Chemistry, The University of North Carolina at Chapel Hill, Chapel Hill, NC 27599, United States

*frankl@email.unc.edu

Table of Contents

General methods and materials

Reagents

δ-valerolactone was dried over calcium hydride, distilled, and stored in a glove box prior to use. *N*-isopropylamide was recrystallized once from a 50/50 mixture of hexanes/toluene prior to use. *n*-butyl acrylate and *N,N*-dimethylacrylamide were passed through an alumina column in order to remove inhibitor prior to use. All other reagents were purchased and used without further purification.

Analysis

Proton nuclear magnetic resonance spectra (^{1}H NMR) were recorded on a Bruker model DRX 400 MHz spectrometer with a solvent resonance as the internal standard (^{1}H NMR: CDCl$_3$ at 7.26 ppm or D$_2$O at 4.79 ppm). UV-Vis spectra were measured on a Gilson 151 UV/VIS Multilength Detector at 254 nm coupled with a Vapourtec R-series recorder.

Gel permeation chromatography (GPC) for poly(*N,N*-dimethylacrylamide) samples were performed on an Agilent 1260 Infinity separation module liquid chromatograph equipped with two Agilent Resipore Columns (PL1113-6300) maintained at 50 °C, and an Agilent 1260 RID G1362A refractive index detector at 50 °C. A solution of 0.1 wt% LiBr in dimethylformamide (DMF) was used as the mobile phase at a flow rate of 1.0 mL/min. Molecular weight and dispersity data are reported relative to poly(ethylene oxide) standards.

For all other polymer samples GPC analysis was performed on a Waters 2695 separations module liquid chromatograph equipped with either four Waters Styragel HR columns (WAT044225, WAT044231, WAT044237, and WAT054460) arranged in series or two Agilent Resipore columns (PL1113-6300) maintained at 35 °C, and a Waters 2414 refractive index detector at room temperature. Tetrahydrofuran was used as the mobile phase at a flow rate of 1.0 mL/min. Molecular weight and dispersity data are reported relative to polystyrene standards.

Viscosity measurements for PEG-water solutions were taken on an ARES-G2 from TA instruments using a concentric cylinder and cup geometry.

Flow geometries

Flow rates for all experiments were calculated by measuring the internal volume of the reactor tubing and dividing by the desired retention time. Listed below are the lengths of tubing used in each experiment.

Experiments	Tubing size	Tubing length	Reactor volume
UV-Vis measurements	0.02 in.	150 cm	304 µL
	0.03 in.	150 cm	684 µL
	0.04 in.	150 cm	1.22 mL
	0.063 in.	150 cm	2.92 mL
	0.093 in.	150 cm	6.57 mL
Poly(δ-valerolactone) polymerizations	0.02 in.	150 cm	304 µL
	0.03 in.	150 cm	684 µL
	0.04 in.	150 cm	1.22 mL
	0.04 in. Droplet	150 cm	1.22 mL
	0.063 in.	20 cm	390 µL
	0.093 in.	30 cm	1.31 mL
	0.093 in. Scale up	900 cm	39.44 mL
Poly (n-butyl acrylate) and poly(N-Isopropylacrylamide) polymerizations	0.04 in.	150 cm	1.22 mL
	0.093 in.	30 cm	1.31 mL
	0.093 in. Scale up	900 cm	39.44 mL
Poly(N,N-dimethylacrylamide) polymerizations	0.04 in.	150 cm	1.22 mL
	0.093 in.	30 cm	1.31 mL
	0.093 in. Scale up	180 cm	7.89 mL

Flow equipment

Flow tubing and connections were purchased from Upchurch Scientific (IDEX Health and Science). Syringe pumps and syringes were purchased from Harvard Apparatus. Luer-lock adapters were purchased to allow withdrawing reaction solution using standard needles (Idex Health and Science).
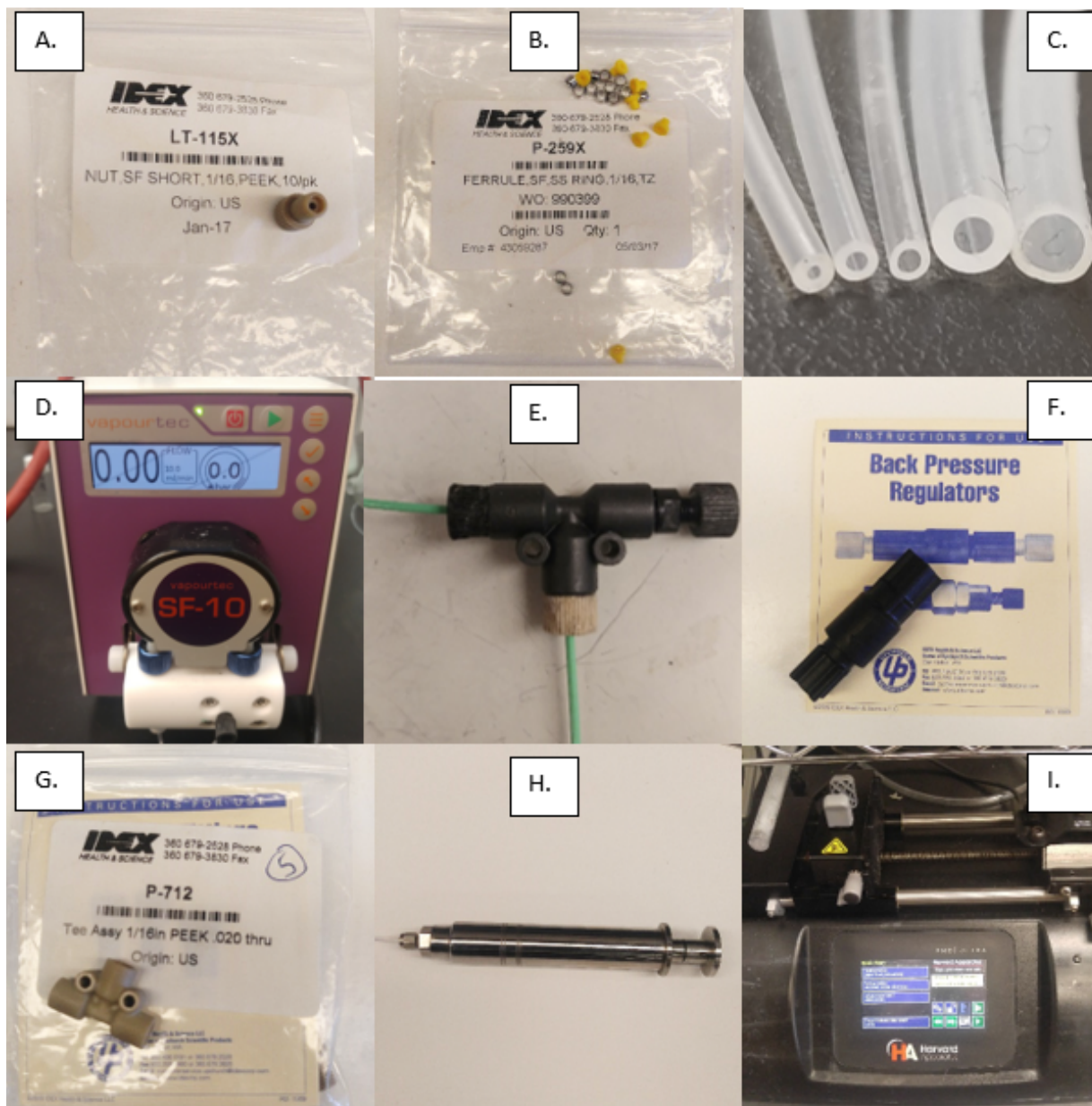

Figure S1. A. PEEK super-flangeless nut **B.** Yellow super-flangeless ferrule with corresponding stainless steel ferrule ring -- sold separately – larger sizes needed for 0.063 and 0.093 in. tubing. **C.** 0.02 in., 0.03 in., 0.04 in., 0.063 in., and 0.093 in. tubing **D.** Vapourtec SF-10 peristaltic pump **E.** Micrometering valve (part number p-445) **F.** back pressure regulator, 40 PSI (part number P-785) **G.** Static mixing Tee **H.** 20 mL stainless steel syringe **I.** Ph.D Ultra syringe pump

Polymerization methodology

Poly(δ-valerolactone) In the glove box using dry reagents and solvents, two solutions were prepared. The first was charged with 0.925 mL (10 mmol) of δ-valerolactone, 0.75 mL of DCM, and a stir bar. The second was charged with 1 mL of DCM, 4.5 mg (0.032 mmol) of triazabicyclodecene, and 10μL (0.080 mmol) of anhydrous 1-hexanol. To initiate the polymerization the two solutions were combined at room temperature and allowed to stir for 10 minutes before being quenched by addition of a small amount of acetic acid. At 100% conversion the target DP is 125 and the target M_n is 12,515.

For flow reactions the solutions were instead loaded into two different syringes that had been dried under vacuum overnight and brought into the glovebox. Outside of the glove box the syringe pumps were set to an identical flow rate with the total rate targeting a 10 minute retention time. A third pump containing an acetic acid/DCM solution was used to quench the reaction. To reach steady state, the pumps were run for 30 minutes (3 retention times) before collecting product.

For scale-up in droplet flow, solutions were prepared inside the glove box in two separate septum caped Erlenmeyer flasks. The peristaltic pumps were set to flow rates slightly lower than predicted for a 10 minute retention time. At first the peristaltic pumps pumped DCM through the system to allow manual adjustment of the argon flow rate until a 10 minute retention time was approximated by visually measuring the velocity of the air bubbles. Once a suitable retention time was estimated the peristaltic pumps began feeding from their respective monomer and catalyst/initiator solutions. When those solutions had been depleted the pumps were switched back to DCM to push the remaining volume of reaction solution through the reactor. During this experiment 100% of material was collected in a single vessel and then further analyzed via NMR and GPC.

Poly(*n*-butyl acrylate)

A single round bottom flask was charged with 28.7 mL (0.2 mol) of deinhibited *n*-butyl acrylate, 98.5 mg (0.6 mmol) of azobisisobutyronitrile, 254 mg (2 mmol) of 2-(2-carboxyethylsulfanylthiocarbonylsulfanyl)propionic acid and 71.3 mL of ethyl acetate. Argon was then bubbled through the solution for 60 minutes. At 100% conversion the target DP is 200 and the target M_n is 25,600 g/mol

For the batch reaction a 2 mL sample was transferred into a small vial pre-purged with Argon and equipped with a stirbar and gas-tight septa. The vial was allowed to stir in a 80°C heat bath for 30 minutes before being quenched by the addition of butylated hydroxytoluene and removal from heat.

For flow reactions the desired length of tubing was submerged in a 80°C heat bath before the solution was loaded into a syringe and the flow rate of the syringe pump was set to target a 30 minute retention time. To reach steady state, the pump was run for 90 minutes (3 retention times) before product was collected in a vial containing a small amount of butylated hydroxytoluene.

For scale-up in droplet flow, the desired length of tubing was submerged in a 80°C heat bath before the peristaltic pump was set to flow rate slightly lower than predicted for a 30 minute retention time. At first ethyl acetate was pumped through the system to allow manual adjustment of the argon flow rate until a 30 minute retention time was approximated by visually measuring the velocity of the air bubbles. Once a suitable retention time was estimated the peristaltic pump began feeding from reaction solution. When that solution had been depleted the pumps were switched back to ethyl acetate to push the remaining volume of reaction solution through the reactor. During this experiment 100% of material was collected in a single vessel and then further analyzed via NMR and GPC.

Poly(*N*-isopropylacrylamide)

A 100 mL volumetric flask was charged with 22.6 g (0.2 mol) of *N*-isopropylacrylamide, 98.5 mg azobisisobutyronitrile, and 254 mg (2 mmol) of 2-(2-carboxyethylsulfanylthiocarbonylsulfanyl)propionic acid. Ethyl acetate was added until the total solution volume reached 100 mL. Argon was then bubbled through the solution for 60 minutes. At 100% conversion the target DP is 200 and the target M_n is 22,600 g/mol. For the batch reaction a 2 mL sample was transferred into a small vial pre-purged with Argon and equipped with a stirbar and gas-tight septa. The vial was allowed to stir in a 100°C heat bath for five minutes before being quenched by the addition of butylated hydroxytoluene and removal from heat.

For flow reactions the desired length of tubing was submerged in a 100°C heat bath before the solution was loaded into a syringe and the flow rate of the syringe pump was set to target a 5 minute retention time. To reach steady state, the pump was run for 15 minutes (3 retention times) before product was collected in a vial containing a small amount of butylated hydroxytoluene.

For scale-up in droplet flow, the desired length of tubing was submerged in a 100°C heat bath before the peristaltic pump was set to a flow rate slightly lower than predicted for a 5 minute retention time. At first ethyl acetate was pumped through the system to allow manual adjustment of the argon flow rate until a 5 minute retention time was approximated by visually measuring the velocity of the air bubbles. Once a suitable retention time was estimated the peristaltic pumps began feeding from reaction solution. When those solutions had been depleted the pumps were switched back to ethyl acetate to push the remaining volume of reaction solution through the reactor. During this experiment 100% of material was collected in a single vessel and then further analyzed via NMR and GPC.

Poly(*N,N*-dimethylacrylamide)

A single vial was charged with 6.15 mL (0.060 mol) of deinhibited *N,N*-dimethylacrylamide, 9.6 mg (0.030 mmol) of 2,2'-azobis[2-(2-imidazolin-2-yl)propane]dihydrochloride (VA-044), 35.7 mg (0.15 mmol) of 2-(butylthiocarbonothioylthio)propanoic acid, 19.2 mL deionized water, and 4.65 mL 1,4-dioxane. The solution was not degassed prior to reacting. At 100% conversion, the target DP is 400 and the target M_n is 39,700 g/mol. For the batch reaction a 2 mL sample was transferred into a small vial pre-purged with Argon and equipped with a gas-tight septa. The vial

was allowed to stir in a 100°C heat bath for 1 minute before being removal from heat and exposed to air to allow quenching.

For the preheated batch reaction, the initiator was separately dissolved at room temperature in 0.2 mL of deionized water and injected into monomer/CTA solution that had been submerged in a 100°C heat bath for two minutes.

For flow reactions the desired length of tubing was submerged in a 100°C heat bath before the solution was loaded into a syringe and the flow rate of the syringe pump was set to target a 1 minute retention time. To reach steady state, the pump was run for 3 minutes (3 retention times) before product was collected in a vial open to air.

For scale-up in droplet flow, the desired length of tubing was submerged in a 100°C heat bath before the peristaltic pump was set to a flow rate slightly lower than predicted for a 1 minute retention time. At first the peristaltic pumps pumped deionized water through the system to allow manual adjustment of the argon flow rate until a 1 minute retention time was approximated by visually measuring the velocity of the air bubbles. Once a suitable retention time was estimated the peristaltic pump began feeding from reaction solution.

Polymerization data not included in the main text

Poly(*N*-isopropylacrylamide)

Reactor geometry	M$_n$ (g/mol)	Đ	Conversion (%)
Batch (2 mL scale)	10900	1.24	79
Flow (0.04 in. tubing)	10800	1.26	75
Flow (0.093 in. tubing)	8900	1.28	67
Droplet (0.093 in. tubing)	9800	1.13	67

The polymerization of *N*-isopropylacrylamide in droplet flow achieved a narrower Đ than batch. We hypothesize that this is due to the loss of control in batch at these higher temperatures. When combined with a back-pressure regulator, the polymerization in flow is better able to maintain control at temperatures well above the solvent's boiling point.

Poly(*N,N*-dimethylacrylamide)

CTA: RAFT CTA, VA-044, H$_2$O, Dioxane, 100°C, 1 min.
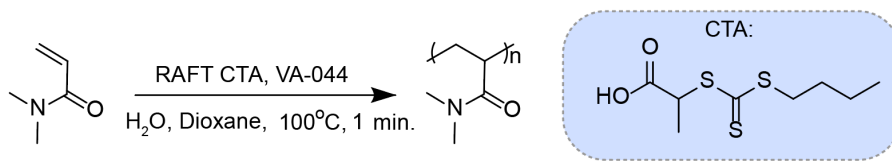
| Reactor geometry	M$_n$ (g/mol)	Đ	Conversion (%)
Batch (2 mL scale)	-	-	6
Pre-heated (2 mL scale)	13800	1.14	89
Flow (0.04 in. tubing)	10200	1.38	64
Flow (0.093 in. tubing)	6700	1.53	38
Droplet (0.093 in. tubing)	12100	1.26	82

For this reaction the rate of heat transfer and mixing played a large role in the conversion of the product. These variables had a larger influence than for other reactions because of the short reaction time, the high specific heat of water, and the need for rapid mixing to facilitate simultaneous initiation. For these reasons it was difficult to discern if the drastically different conversions are due to RTD effects or different rates of mixing and heat transfer in each geometry.

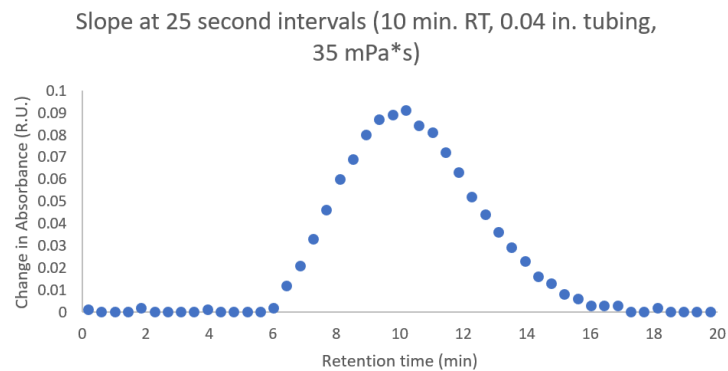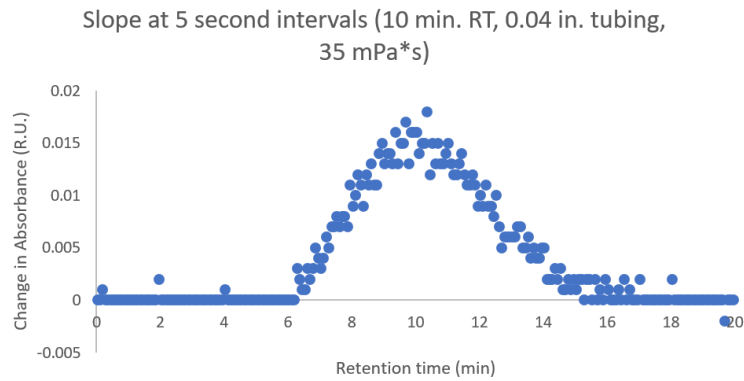# Sample residence time distribution visualization

Raw UV-vis data was collected from the recorder as a number of discrete data points.

Raw UV-vis data (10 min. RT, 0.04 in. tubing, 35 mPa*s)
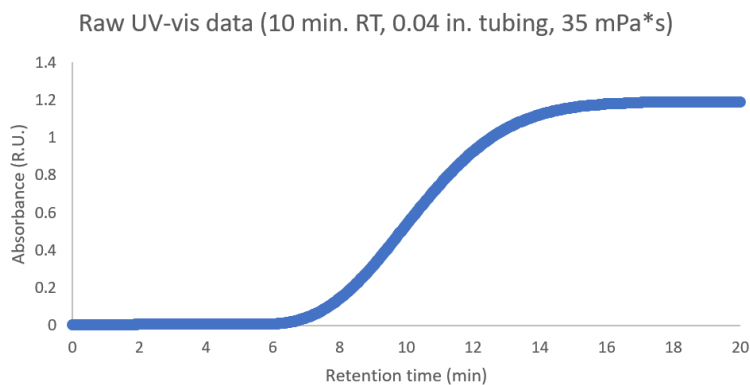
The slope cannot be directly found using the first derivative because the raw data is a number of discrete points rather than a continuous function. Instead slope of each data point is measured by the ratio of change in y-axis and change in x-axis. The instrument makes measurements every second so the slope is calculated from the change in absorption per every one second period.

Slope at 1 second intervals (10 min. RT, 0.04 in. tubing, 35 mPa*s)
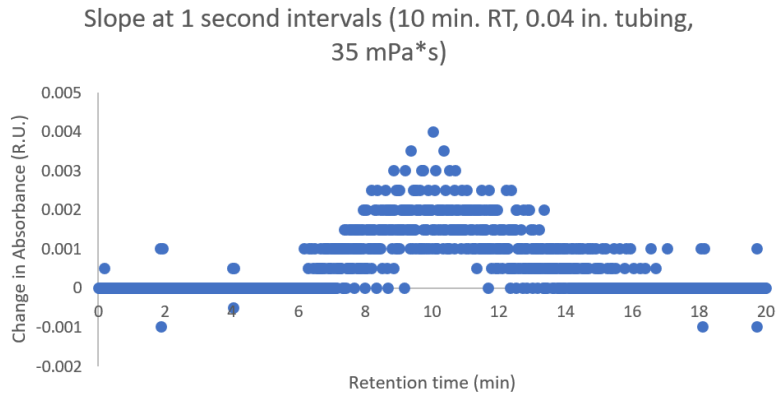
As seen above, the data doesn't represent the RTD in an easy to interpret manner. This is due to the change in absorbance per second being very small. To fix this problem multiple data points are summed together, resulting in the change in absorbance per 5 seconds, 10 seconds or longer.

Slope at 5 second intervals (10 min. RT, 0.04 in. tubing, 35 mPa*s)

Slope at 25 second intervals (10 min. RT, 0.04 in. tubing, 35 mPa*s)

Once a good interval for averaging the slopes is determined we normalize the data on both the x and y axis. Normalizing the x-axis requires first finding the mean retention time. For a symmetric curve, is as simple as finding the time point that corresponds to half of the total change in absorbance.

9

Raw UV-vis data (10 min. RT, 0.04 in. tubing, 35 mPa*s)
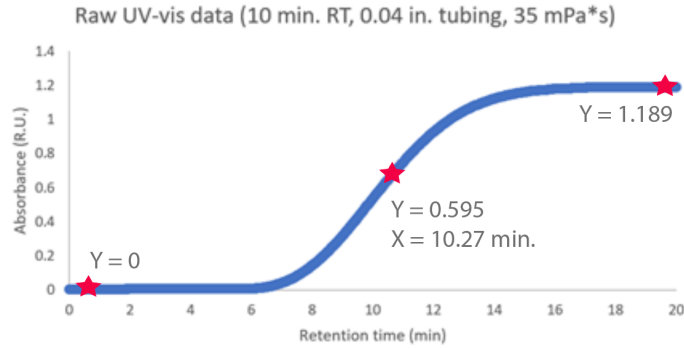
In this experiment the mean residence time was found to be 10.27 minutes. This is higher than the 10-minute predicted residence time due to dead volume between the reactor and the detector. In order to normalize the RTD, the X-axis was divided by the mean residence time and the Y-axis was divided such that the total area under the curve was equal to one. This allows the direct comparison of different RTD's even at different residence times or using different numbers of averaged points.